DALTON
FULL PAPER

Metal ion co-ordination of a tripodal imidazole-derivative and its tridentate constituent: equilibrium and structural studies †

Attila Jancsó,[a] Ibolya Török,[b] László Korecz,[c] Antal Rockenbauer[c] and Tamás Gajda *[a]

[a] *Department of Inorganic and Analytical Chemistry, University of Szeged, H-6701 Szeged, P.O. Box 440, Hungary. E-mail: tamas.gajda@chem.u-szeged.hu*
[b] *Research Group on Biocoordination Chemistry of the Hungarian Academy of Sciences, University of Szeged, H-6701 Szeged, P.O. Box 440, Hungary*
[c] *Chemical Research Center, Institute of Chemistry, H-1525 Budapest, P.O. Box 17, Hungary*

Received 11th December 2001, Accepted 15th April 2002
First published as an Advance Article on the web 17th May 2002

A new unsymmetric imidazole based tripodal ligand with different arm lengths (*N*,*N*′-bis(imidazole-4-ylmethyl-5-methyl)histamine, bimhm), its tridentate constituent (*N*-(imidazole-4-ylmethyl-5-methyl)histamine, imhm) and a related ligand (*N*-methyl-*N*′-(2-ylmethylpyridine)ethylenediamine, pyrdiam) not containing an imidazole unit have been synthesized. Equilibrium and solution structure of their copper(II) and zinc(II) complexes have been investigated by pH-metry, UV/VIS, EPR and ^{1}H NMR spectroscopy as structural models of metal-binding multi-imidazole motifs of metalloproteins. Several mono- and bis-complexes having different protonation states are formed, except for the zinc(II)–bimhm system, where only mono-complexes have been detected. Most of these species possess (distorted) octahedral geometry, but a pentaco-ordinated structure is preferred in the $[ML]^{2+}$ complexes of bimhm. The spectroscopic data indicate a square pyramidal geometry for $[Cu(bimhm)]^{2+}$, while a trigonal bipyramidal structure is proposed for $[Zn(bimhm)]^{2+}$. The deprotonation of the complex $[Cu(imhm)]^{2+}$ results in an imidazolate-bridged $[Cu(imhmH_{-1})]_n^{n+}$ oligomer, while in the absence of such a bridging unit, the hydroxo-mixed $[CuL(OH)]^+$ complex is formed with pyrdiam.

Introduction

Metal complexes of a wide variety of imidazole-based ligands have been studied as structural and/or functional models of several metalloproteins.[1–16] These studies were focused mainly on the solid state structure of the obtained metal complexes,[1–10] but their speciation and solution structure have also been studied in some cases.[11–16] Bis-, tris- and tetraimidazole compounds provided the possibility to study the intrinsic co-ordination properties of multiimidazole environments.[10,12,14–16] The stability of the species increased parallel with the increasing number of imidazole rings, but the distortion from the ideal geometry also showed a similar trend due to the more and more strained ligand-backbone.

The presence and/or position of additional nitrogen- and/or oxygen-donors, beside the imidazole rings, has been found to alter strongly the structure and properties of their complexes. Tripodal ligands are especially suitable to assess the electronic and geometrical factors regulating the copper containing proteins. Consequently, a number of investigations have been devoted to study of the structure of copper(II) complexes of different tetra- or polydentate imidazole-based tripodal ligands.[1–7,15] Tetradentate tripodal ligands generally form a pentaco-ordinated structure with an additional water molecule or counter ion, but the actual structure (square pyramidal or trigonal bipyramidal) strongly depends on the properties of the ligands, *e.g.* nature of the donor groups and counter ions, symmetry of the ligand or the constitution of the arms. Though the solid state structures of such complexes are well established,[1–7] and solution structural data are also available for some complexes in different solvents,[1,3–6] complete solution chemical characterisation, which is essential for the full co-ordination chemical description, has been performed very rarely.[12] A large portion of the investigated tripodal ligands are either symmetric or the donor groups are of the same distance from the central atom, except for some pyridyl/thioether and pyridyl/amine containing compounds.[17–20] Unsymmetric tripodal ligands, providing fused chelate rings with different ring-size,[17–20] may be of great interest, since they generally form square pyramidal complexes[4] mimicking the structure detected in the active center of many copper(II) proteins.[21]

As a continuation of our work on metal complexes of polydentate imidazole-ligands,[11–14] here we present equilibrium and solution structural studies of copper(II) and zinc(II) complexes formed with an unsymmetric tripodal ligand having $–CH_2–$ and $–CH_2–CH_2–$ groups as "spacers" between the central amino group and imidazole rings (bimhm), with its tridentate constituent (imhm) and a related tridentate ligand not containing an imidazole ring (pyrdiam), as potential structural models of metal binding sites of metalloproteins.

Experimental

Materials

Copper(II) and zinc(II) perchlorate (Fluka) solutions were standardized complexometrically. pH-metric titrations were performed by NaOH (Fluka) standard solution. Histamine dihydrochloride (Sigma), 4-methyl-5-imidazolecarboxaldehyde (Aldrich), *N*-methylethylenediamine (Sigma) and pyridine-5-carboxaldehyde (Sigma) were used without further purification.

† Electronic supplementary information (ESI) available: Fig. S1. Electronic absorption spectra of the main species formed in the imhm–Cu(II) system. Fig. S2. UV/VIS spectra of the Cu(II)–imhm 1 : 1 system. Description of the Cu(II)–pyrdiam system. Table S1. p*K* values of pyrdiam and formation constants of its Cu(II) complexes. Table S2. Spectroscopic data for the Cu(II)–pyrdiam complexes. Fig. S3. EPR spectra of the Cu(II)–pyrdiam system. See http://www.rsc.org/suppdata/dt/b1/b111275a/

This journal is © The Royal Society of Chemistry 2002

Synthesis of the ligands

a, *N*-(Imidazole-4-ylmethyl-5-methyl)histamine·3HCl (imhm·3HCl). Histamine dihydrochloride (1.841 g, 10 mmol) was dissolved in 30 mL dry ethanol and neutralized by the appropriate amount of 1 M KOH dissolved in ethanol. After 0.5 h stirring the precipitated KCl salt was filtered off. 4-Methyl-5-imidazolecarboxaldehyde (1.101 g, 10 mmol) dissolved in 20 mL ethanol was then added to the filtered solution of histamine. The mixture was stirred for 2 h, the formation of the Schiff-base during the reaction was followed by TLC. Palladium on activated charcoal (Fluka) as catalyst was added to the solution very carefully. For the reduction of the Schiff-base H_2 gas was bubbled through the solution for 5 h until the reaction was completed. The volume of the solution was kept constant by adding ethanol. After finishing the reduction procedure HCl gas was bubbled through the clean, yellowish solution for approx. 15 min. The solution was then evaporated, the white powder product was filtered off and recrystallised from ethanol. Yield: 2.25 g, 71.5%. The structure and purity was demonstrated by NMR spectroscopy and potentiometry. ^{1}H NMR (in water): δ = 8.604 (s, 1 H, C^2_{hm}**H**), 8.604 (s, 1 H, C^2_{im}**H**), 7.330 (s, 1 H, C^5_{hm}**H**), 4.388 (s, 2 H, im-C**H**$_2$–NH), 3.418 and 3.171 (t and t, ^3J = 7.56 Hz, 2 H and 2 H, NH–C**H**$_2$–C**H**$_2$–hm), 2.345 (s, 3 H, C**H**$_3$–im).

b, *N*,*N*′-Bis(imidazole-4-ylmethyl-5-methyl)histamine·4HCl (bimhm·4HCl). Histamine dihydrochloride (0.921 g, 5 mmol) was dissolved in 30 mL dry methanol and neutralized by the appropriate amount of 1 M NaOH (in MeOH), then 4-methyl-5-imidazolecarboxaldehyde (1.101 g, 10 mmol) in 30 mL dry methanol was added. To this mixture 1 g sodium borohydride was added in small portions while stirring. After stirring for 48 h at room temperature the reaction was completed by refluxing for 12 h. The solution was then acidified with concentrated hydrochloric acid. The precipitate was filtered, the solution was reduced to 2–3 mL and 30 mL methanol was added. The precipitate was filtered off again. The solution was evaporated to dryness by codistillation with absolute ethanol. The crude product was recrystallised from methanol. Yield: 1.47 g, 66%. The structure and purity was confirmed by NMR spectroscopy and potentiometry. ^{1}H NMR (in water): δ = 8.497 (d, ^4J ~0.8 Hz, 1 H, C^2_{hm}**H**), 8.468 (s, 1 H + 1 H, C^2_{im}**H**), 7.125 (s, broad, 1 H, C^5_{hm}**H**), 3.813 (s, 2 H + 2 H, im-C**H**$_2$–NH), 2.890 (m, 2 H + 2 H, NH–C**H**$_2$–C**H**$_2$–hm), 2.213 (s, 6 H, C**H**$_3$–im).

pH-metric measurements

The protonation and co-ordination equilibria were investigated by potentiometric titration in aqueous solution (I = 0.1 M, $NaClO_4$ and/or NaCl, and T = 298 ± 0.1 K) using an automatic titration set including a Dosimat 665 (Metrohm) autoburette, an Orion 710A precision digital pH-meter and an IBM-compatible PC. The Orion 8103BN semimicro pH glass electrode was calibrated[22] *via* the modified Nernst equation (1):

$$E = E_0 + K\log[H^+] + J_H[H^+] + \frac{J_{OH}K_W}{[H^+]} \quad (1)$$

where J_H and J_{OH} are fitting parameters in acidic and alkaline media for the correction of experimental errors, mainly due to the liquid junction and to the alkaline and acidic errors of the glass electrode; $K_W = 10^{-13.75}$ M^2 is the autoprotolysis constant of water.[23] The parameters were calculated by a non-linear least squares method. The complex formation was characterized by the following general equilibrium process (2):

$$pM + qL + rH \xleftrightarrow{\beta_{M_pL_qH_r}} M_pL_qH_r \quad (2)$$

$$\beta_{M_pL_qH_r} = \frac{[M_pL_qH_r]}{[M]^p[L]^q[H]^r} \quad (3)$$

where M denotes the metal ion and L the non-protonated (neutral) ligand molecule. The corresponding formation constants ($\beta_{M_pL_qH_r} \equiv \beta_{pqr}$) were calculated using the computer program PSEQUAD.[24]

The protonation and complex formation constants were determined from 4–10 independent titrations (60–90 data points per titration). The metal-to-ligand ratios varied between 1 : 1 and 1 : 3, with the metal ion concentration between 4.9×10^{-4} and 4.2×10^{-3} mol dm^{-3}.

Electronic absorption, EPR and NMR measurements

UV-VIS spectra were measured on a Hewlett Packard 8452A diode array spectrophotometer. The individual spectra of the copper(II) complexes formed were calculated by the previously mentioned computer program PSEQUAD. The EPR spectra were recorded on a JEOL-JES-FE 3X spectrometer in the X-band region at 298 and 77 K with 100 kHz field modulation. Manganese(II)-doped MgO powder was used as field standard. The concentration of copper(II) was 4–5 × 10^{-3} mol dm^{-3}. The EPR parameters were calculated by a computer program able to handle four (but preferably two) coexisting species.[25] ^{1}H NMR measurements were performed on a Bruker Avance DRX 500 spectrometer. The chemical shifts δ were measured with respect to dioxane as internal reference and converted relative to $SiMe_4$, using $\delta_{dioxane}$ = 3.70. The zinc(II) and ligand concentrations were 0.006 and 0.006–0.012 mol dm^{-3}, respectively. Measurements were generally made in H_2O–D_2O (9 : 1).

Results and discussion

Protolysis of the ligands

The protolysis equilibria of the ligands have been studied between pH 2–11. The determined pK values are listed in Table 1. Imhm is fully protonated at pH 2 and deprotonates in three separate steps. The first two steps are slightly overlapped and can possibly be attributed to the deprotonation of the two imidazole groups (Scheme 1). The first deprotonation process

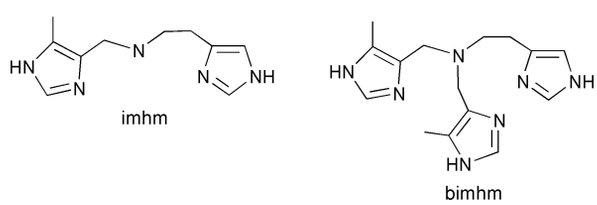

Scheme 1 Schematic structure of the ligands studied.

of bimhm takes place below the pH range studied. The enhanced acidity of one of the three imidazole moieties is very likely the result of the formation of an intramolecular hydrogen bond within the LH_3^{3+} species. Such interaction might be preferred between the two identical –CH_2–Im arms. As a result of that, the following pK value is remarkably shifted to higher pH as compared with the first pK of imhm. The values of pK_2 and pK_3 reflect strong overlapping of the deprotonation processes. The highest pK value can be attributed to the deprotonation of the secondary/ternary ammonium group in both cases.

Copper(II) and zinc(II) complexes of imhm and pyrdiam

Using $NaClO_4$ as background electrolyte, precipitation was detected in the case of imhm in the presence of both metal ions at pH 7.4 (equimolar solution) or at ≈8.5 (ligand excess). With NaCl as background salt, the measuring pH range could be extended up to pH 9.7 (1 : 1 systems) or 10.2 (ligand excess) in the case of copper(II), and thus the detection of a further complex formation process became possible. Changing the background electrolyte does not increase the solubility of zinc(II) complexes. The overall formation constants together with some derived data are listed in Table 1. The complexes $[ML]^{2+}$ are

Table 1 pK-values of the ligands and formation constants (β) of their copper(II) and zinc(II) complexes (as their logarithms, the estimated errors are in parentheses), $I = 0.1$ M NaCl, $T = 298$ K

Species	imhm		bimhm	
pK_1	4.70(1); [a]4.76(1)		<1.5	
pK_2	6.10(1); [a]6.14(1)		5.86(4)	
pK_3	9.09(1); [a]9.10(1)		6.59(4)	
pK_4	—		8.61(3)	
	copper(II) [b]	zinc(II) [a]	copper(II)	zinc(II)
MLH_2	—	—	22.10(7)	—
MLH	16.4(1)	12.75(5)	20.15(3)	16.0(1)
ML	14.79(1)	8.28(1)	16.06(3)	12.73(2)
MLH_{-1}	5.51(7)	—	—	—
$M_4L_4H_{-4}$	31.6(1)	—	—	—
ML_2H_2	—	—	33.6(1)	—
ML_2H	26.2(1)	19.6(1)	27.63(9)	—
ML_2	18.60(5)	11.79(5)	19.96(7)	—
[c]pK_{MLH}	1.61	4.47	4.09	3.27
[c]pK_{ML_2H}	7.60	7.81	7.67	—
log K_2	3.81	3.51	3.90	—
log(K_1/K_2)	10.98	4.77	12.16	—
Fitting parameter (cm^3)	0.008	0.005	0.004	0.007
Number of exp. points	679	328	369	290

[a] $I = 0.1$ mol dm^{-3} $NaClO_4$. [b] log β values for the imhm–Cu(II) species in 0.1 mol dm^{-3} $NaClO_4$ medium are as follows: MLH, 17.10(3); ML, 14.92(1); ML_2H, 26.60(9); ML_2, 19.08(5). [c] $pK_{ML_mH_n} = \log\beta_{ML_mH_n} - \log\beta_{ML_mH_{n-1}L}$.

dominant over a wide pH-range in the equimolar systems (Fig. 1A), preceded by the formation of $[MLH]^{3+}$ species in a small amount. The formation of $[Cu(imhm)]^{2+}$ starts at *ca.* two units lower pH than that of $[Zn(imhm)]^{2+}$, corresponding with the difference in their formation constants (Table 1). Around pH 8.8 a further deprotonation was observed in the presence of copper(II) (and NaCl as background electrolyte). Differently protonated bis-complexes are also formed above pH 5 (Fig. 1B)

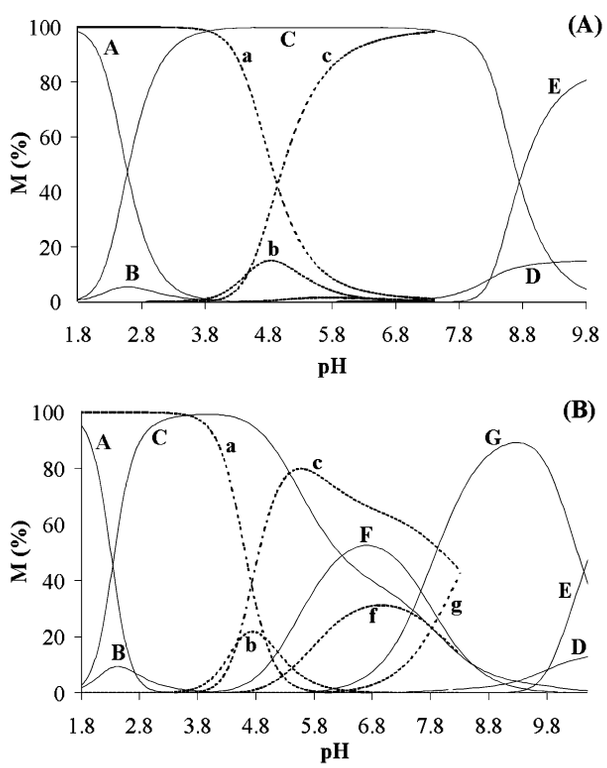

Fig. 1 Species distribution in the copper(II)–imhm (continuous line, upper case letters) and zinc(II)–imhm (dotted line, lower case letters) systems, at [M]/[L] = 1 : 1 (**A**) and 3 : 1 (**B**). ([Cu^{2+}], [Zn^{2+}] = 0.005 mol dm^{-3}, $T = 298$ K, $I = 0.1$ mol dm^{-3} NaCl (Cu^{2+}) and $NaClO_4$ (Zn^{2+})). M (A,a), MLH (B,b), ML (C,c), MLH_{-1} (D), $M_4L_4H_{-4}$ (E), ML_2H (F,f), ML_2 (G,g), charges are omitted for simplicity.

in the case of ligand excess. The log(K_1/K_2) value for copper(II) is much higher than for zinc(II) (10.98 and 4.77, respectively), reflecting the higher preference of regular octahedral symmetry in the latter case. To obtain strucural information on the copper(II) complexes, combined pH-metric-spectrophotometric and EPR measurements were performed. The individual spectroscopic parameters of the complex $[Cu(imhm)]^{2+}$ (Table 2) are consistent with 3N co-ordination in the equatorial plane of copper(II) (*e.g.* the estimated[26] λ^{d-d}_{max} value for {NH_2,$2N_{im}$, H_2O} co-ordination in a distorted octahedron is 625 nm). The deprotonation of this species yields important, but concentration dependent, blue shift of the d–d transition band (Table 2 and Figure S1, ESI †). This indicates the formation of at least two species, existing in equilibrium. To verify this observation spectrophotometric titrations have been performed in the equimolar solution of imhm and copper(II) at constant pH (9.6) with variation of the total concentrations (see Figure S2, ESI †). Dilution caused a significant shift of the d–d transition band towards the lower energies, from 562 to 598 nm. At the higher end of the applied concentration range ([Cu^{2+}] = [imhm] = 5 mM), the deprotonation of $[Cu(imhm)]^{2+}$ results in a considerable decrease of EPR signal intensity (Fig. 2A), which

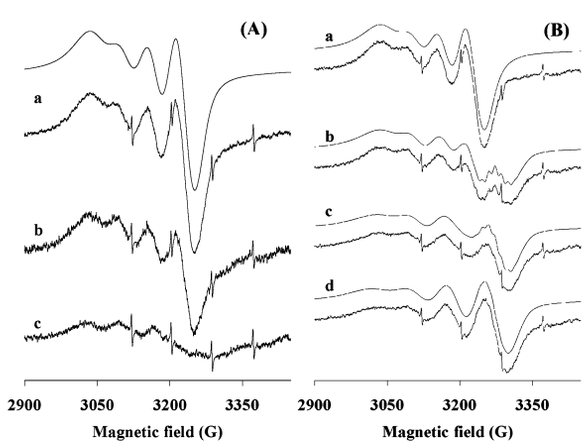

Fig. 2 Experimental and simulated EPR-spectra of the imhm–copper(II) 1 : 1 (**A**) and 3 : 1 (**B**) systems. pH = 6.63 (a), 8.68 (b), 9.47 (c) (**A**) and 4.11 (a), 5.89 (b), 7.64 (c) and 9.21 (d) (**B**). [L] = [M] = 0.005 M (**A**), [L] = 3 × [M] = 0.015 M (**B**), $T = 298$ K.

Table 2 Spectroscopic data for the copper(II) complexes of the studied ligands

Ligand	Complex	g_0	A_0/G	$a_{N,0}$G	$g_\perp$	$g_\parallel$	$A_\parallel$/G	λ_{max}/nm [ε]/M^{-1} cm^{-1}
imhm	ML	2.124	55.4	10.5	2.060	2.237	167.7	635 [59]
	[a]MLH_{-1}	—	—	—	—	—	—	598 [88]
	[b]$M_4L_4H_{-4}$	—	—	—	—	—	—	562 [345]
	ML_2H	2.108	72.8	13.2	2.053	2.224	187.1	574 [109]
	ML_2	2.112	72.3	12.6	2.057	2.233	180.5	594 [86]
bimhm	MLH	2.124	47.4	10.5	—	—	—	652 [93]
	ML	2.137	37.0	—	2.065	2.277	134.0	728 [54]
							$A_\perp = -16.0$	≈900 [52]
	[c]ML_2H_2							—
	[c]ML_2H	[c]2.126	[c]64.2	[c]11.2	[c]2.06	[c]2.25	[c]153	686 [90]
	[c]ML_2							660 [82]

[a] Parameters could not be determined for $CuLH_{-1}$ due to its small concentration. [b] EPR silent species. [c] Due to the similar environment of copper(II) in the bis-complexes, EPR spectra did not show measurable differences between the three bis-species and they were handled as one using the sum of their concentrations.

corresponds to the formation of dimer or oligomer species with strong antiferromagnetic interaction between the metal centres. The lower concentration range ($[Cu^{2+}] < 1$ mM) is not accessible by EPR spectroscopy.

The formation of several species can be taken into account to explain the above observations. The most obvious is the formation of a hydroxo-mixed complex $[Cu(imhm)(OH)]^+$ which undergoes a dimerization at higher concentration, through the metal-bound hydroxide ions. However, the formation of such a μ-dihydroxo-bridged complex $[Cu_2(imhm)_2(OH)_2]^{2+}$, which would have a pentaco-ordinated structure, cannot explain the 70 nm blue shift of the d–d transition, observed at higher concentrations. The spectral change reflects rather the co-ordination of a fourth nitrogen in the equatorial plane of copper(II). This is made possible by the formation of an imidazolate-bridged cyclic oligomer $[Cu(imhmH_{-1})]_n$, as was earlier reported for several related histamine or histidine containing di-[27–29] and tripeptides,[30] or imidazole containing Schiff-bases.[31] The bridging units are probably the less substituted histamine-like imidazole rings. During the data evaluation we considered a tetrameric complex, since at least four monomeric units are needed to form a closed loop,[27–29,31] but the formation of higher oligomers cannot be excluded.[29] At lower concentrations, the mononuclear $[CuLH_{-1}]^+$ is the dominant species. By analogy with the related systems,[25–28] this is most likely a hydroxo-mixed complex, which is also supported by the λ^{d-d}_{max} value calculated for this species (the expected[26] value for a $\{NH_2,2N_{im},OH^-\}$ co-ordination is 590 nm). In this way the mentioned complex is better described as $[Cu(imhm)(OH)]^+$. The log K value for the oligomerization process ($[CuLH_{-1}]^+ = 1/4[(MLH_{-1})_4]^{4+}$, log $K = 2.39$) is close to the values reported earlier for the related equilibria (log $K = 1.8$–2.3).

To find further evidence for the above mentioned equilibrium, we studied the copper(II) complexes of a related tridentate ligand (*N*-methyl-*N′*-(2-ylmethylpyridine)ethylendiamine) containing a pyridine ring and an amino group instead of the two imidazole rings of imhm, where only monomeric complexes have been detected (see ESI †). Consequently, the oligomerization process, observed for imhm, is clearly the result of the presence of the imidazole rings, and proceeds through the formation of imidazolate bridges.

The spectral parameters of $[Cu(imhm)(imhmH)]^{3+}$, formed in presence of ligand excess, are considerably different from those of $[Cu(imhm)]^{2+}$, and correspond to four equatorial nitrogen co-ordination in a distorted octahedral geometry (*e.g.* the estimated[26] λ^{d-d}_{max} value for a $\{NH_2,3N_{im}\}$ co-ordination is 577 nm). The 20 nm red shift of the d–d transition, the slightly larger g and smaller A (a_0) values of $[CuL_2]^{2+}$ (Table 2) as compared with $[CuL_2H]^{3+}$, as well as the value of pK_{ML_2H} which is 1.5 logarithmic units lower than the pK_3 of imhm (Table 1), indicate axial nitrogen co-ordination in $[CuL_2]^{2+}$. Indeed, the ethyl-arm of the histamine-like imidazole ring allows the more elongated axial co-ordination, and the formation of 5N or 6N co-ordinated $[CuL_2]^{2+}$ species. Although the high $\log(K_1/K_2)$ value (10.93, Table 1) would suggest a different binding mode of the second ligand, such a difference may arise from the structural rearrangement within the complex too (*i.e.* the histamine-like imidazole ring of the first ligand moves from an equatorial position to an axial one during the process $[ML]^{2+} + L = [ML_2]^{2+}$).

^{1}H NMR spectra were collected to characterize the zinc(II) complexes of imhm. The spectral variation of imidazole protons as a function of pH and zinc(II) concentration is presented in Fig. 3. The observed chemical shifts are depicted in Table 3.

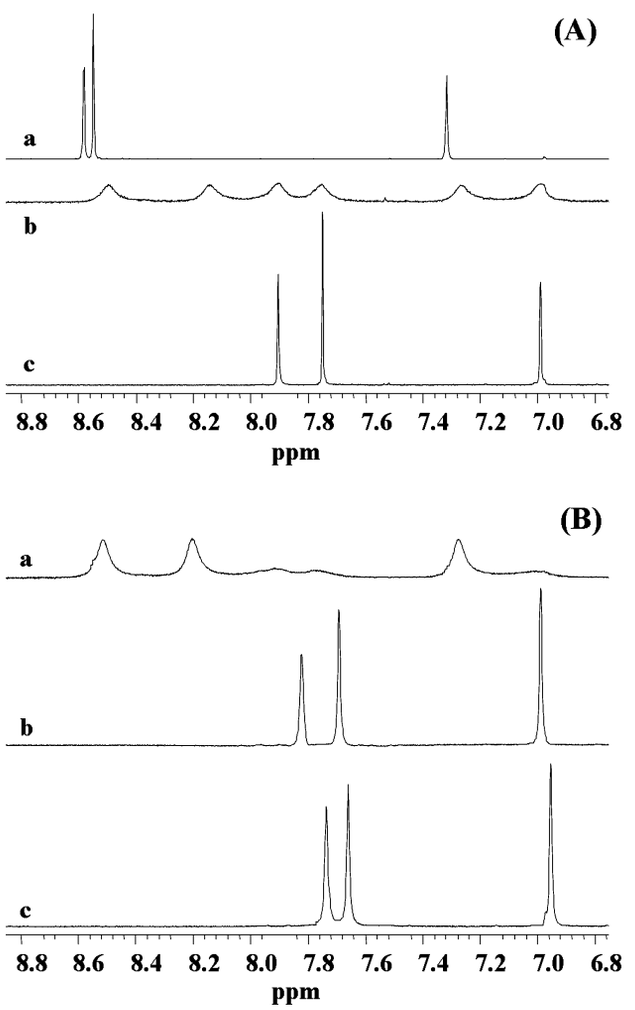

Fig. 3 Parts of the ^{1}H NMR spectra measured in the imhm–zinc(II) system. (**A**): [L] = [M] = 0.006 M, pH = 3.71 (a), 4.75 (b) and 6.90 (c). (**B**): [L] = 2 × [M] = 0.012 M pH = 4.74 (a), 6.90 (b) and 8.00 (c).

Table 3 ^{1}H NMR chemical shifts of imhm and bimhm in ppm measured for the free ligand and in the zinc(II) : L 1 : 1 systems at T = 298 K

System	pH	$C^2_{hm}H$	$C^2_{im}H$	$C^5_{hm}H$	im–CH_2–NH	NH–CH_2–CH_2–hm	CH_3–im
imhm	6.90	7.763	7.627	6.996	4.100	3.252, 2.939 [b]	2.190
[a]imhm	11.30	7.601	7.513	6.820	3.590	2.718 [c]	2.094
imhm–Zn(II)	6.90	7.901	7.748	6.989	— [d]	— [d]	2.138
bimhm	6.80	7.849	7.805	6.909	3.987	3.126, 2.897 [e]	2.137
[a]bimhm	11.30	7.568	7.546	6.714	3.552	2.702 [c]	2.057
bimhm—Zn(II)	6.80	7.993 [f]	7.802	6.979	3.792, 3.624 [g]	2.904, 2.734 [h]	2.136

[a] Fully deprotonated ligands. [b] Two triplets, ^3J = 7.3 Hz. [c] Multiplet. [d] Very broad signals in the 4–2.6 ppm range, assignation is not possible. [e] Two triplets, ^3J = 7.3 Hz. [f] Four bond coupling with C^5_{hm}**H**, ^4J = 1.4 Hz. [g] AB quartet, ^2J = 14.9 Hz. [h] Two slightly distorted triplets, $^3J \approx$ 5.3 Hz.

In both equimolar solution and in the presence of a two fold ligand excess, two sets of peaks appeared at pH = 4.75, indicating slow ligand exchange, on the NMR timescale, of the formed $[Zn(imhm)]^{2+}$ complex. All signals of the bound ligand are strongly upfield shifted, indicating the tridentate co-ordination of imhm in $[ZnL]^{2+}$. However, in the presence of a two fold ligand excess, only one set of signals can be seen at pH 6.9, where $[ZnL]^{2+}$ (≈60%), $[ZnL_2H]^{3+}$ (≈40%) and free ligand (HL^+) are present, which refers to fast mutual ligand exchange. The explanation of the increasing ligand exchange rate with increasing pH is not obvious, but is probably related to the strong intra- and/or intermolecular hydrogen bonding network of the free ligand at pH 4.75 (in H_2L^{2+} and H_3L^{3+}), which should collapse during the complex formation.

Copper(II) and zinc(II) complexes of bimhm

The pH-metric data were evaluated up to pH 8.3 and 7.5–9.0 for the zinc(II) and copper(II) containing systems, respectively, since precipitation occurred at higher pH. The determined formation constants are collected in Table 1, representative speciation curves are depicted in Fig. 4. In the presence of copper(II), the diprotonated $[Cu(imhmH_2)]^{4+}$ is the first-formed species in the acidic pH range. The monoprotonated $[Cu(imhmH)]^{3+}$ complex becomes dominant around pH 3. Its transformation into $[Cu(imhm)]^{2+}$ ($[CuLH]^{3+} = [CuL]^{2+} + H^+$) can be described with a pK of 4.09. In the analogous zinc(II) containing system, the speciation is rather different. The complex ZnLH is only a minor species, since its deprotonation takes place at nearly one unit lower pH (pK = 3.26) as compared with the corresponding copper(II) complex. These data clearly show the preference of tridentate 3N co-ordination of bimhm to copper(II) over zinc(II), while the tetradentate co-ordination of the ligand is more favoured in the case of zinc(II). The preferred formation of the monoprotonated $[CuLH]^{3+}$ complexes has also been reported with some unsymmetric, tripodal polyamine ligands having one or more propyl arm(s).[19]

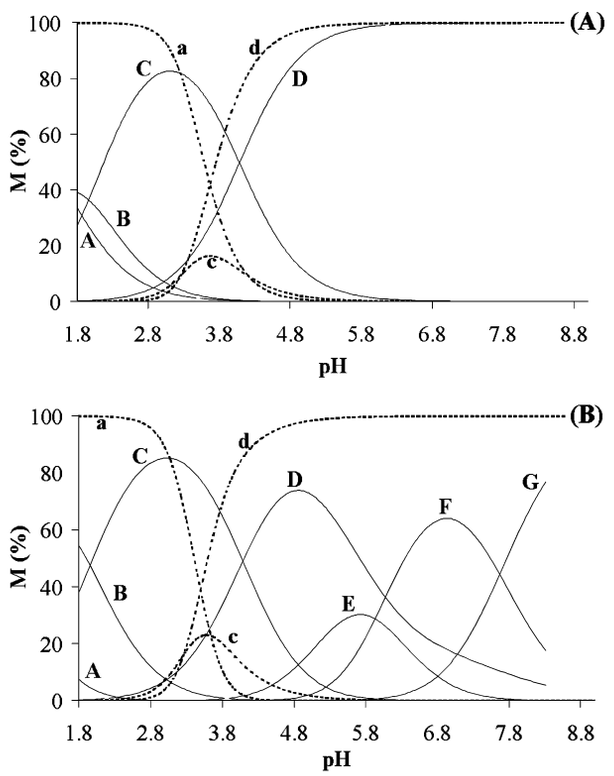

Fig. 4 Species distribution in the copper(II)–bimhm (continuous line, upper case letters) and zinc(II)–imhm (dotted line, lower case letters) systems, at [M]/[L] = 1 : 1 (**A**) and 3 : 1 (**B**). ($[Cu^{2+}]$, $[Zn^{2+}]$ = 0.005 mol dm^{-3}, T = 298 K, I = 0.1 mol dm^{-3} NaCl). M (A,a), MLH_2 (B), MLH (C,c), ML (D,d), ML_2H_2 (E), ML_2H (F), ML_2 (G), charges are omitted for simplicity.

In the presence of a ligand excess, no bis-complexes were detected with zinc(II), but surprisingly such species are formed with copper(II) (Fig. 4B). The formation of $[CuL_2H_x]^{(2+x)+}$ species were not reported in earlier solution equilibrium studies on copper(II) complexes of tetradentate tripodal ligands, mostly derivatives of tren (tris(2-aminoethyl)amine) or trpn (tris(3-aminopropyl)amine).[19,20] However, our data clearly indicate their presence with bimhm. This notable difference between the copper(II)–bimhm and the earlier reported systems, as well as between the copper(II)– and zinc(II)–bimhm complexes, may suggest different geometrical preferences. Therefore, solution structural data have been collected by EPR, UV/VIS and ^{1}H NMR measurements in the case of copper(II) and zinc(II), respectively.

The spectroscopic data of the complex $[Cu(bimhmH)]^{3+}$ (Table 2) are close to those found for $[Cu(imhm)]^{2+}$, indicating similar 3N co-ordination. Its deprotonation around pH 4 strongly suggests 4N co-ordination in the complex $[Cu(bimhm)]^{2+}$. The EPR parameters of the latter species, especially the small a_0 and $A_\parallel$ and the negative $A_\perp$ hyperfine component, indicate a notable change of geometry parallel with the deprotonation and co-ordination of the fourth donor group (Fig. 5, Table 2) and reflect a non-tetragonal symmetry. (The negative $A_\perp$ value originates from the $A_0 = 1/3(A_\parallel + 2A_\perp)$ relation.) The results of the combined pH-metric-spectrophotometric titrations also support the above mentioned geometrical change. The individual spectrum of the $[CuL]^{2+}$ complex of bimhm (Fig. 6) displays two d–d bands, at 728 and 900 nm, typical for species with pentaco-ordinated, square planar (sp) or trigonal bipyramidal (tbp) structures.[1,3,4,19,33–36] The nearly equal intensity of the two bands may indicate intermediate geometry between sp and tbp.[35,36] Trigonal bipyramidal copper(II) comples are known to have "reversed" axial EPR appearance[1,4,32–34] while square-pyramidal species display a typical tetragonal (axial) pattern.[1,35,36] Based on the above observations, the spectroscopic data of the $[Cu(bimhm)]^{2+}$ complex indicate a distorted pentaco-ordinated structure, close to a square pyramid.

Three different protonation states ($[CuL_2H_x]^{(2+x)+}$, x = 0–2) have been identified for the bis-complexes (Fig. 4B). The equilibrium constants for the co-ordination of the differently

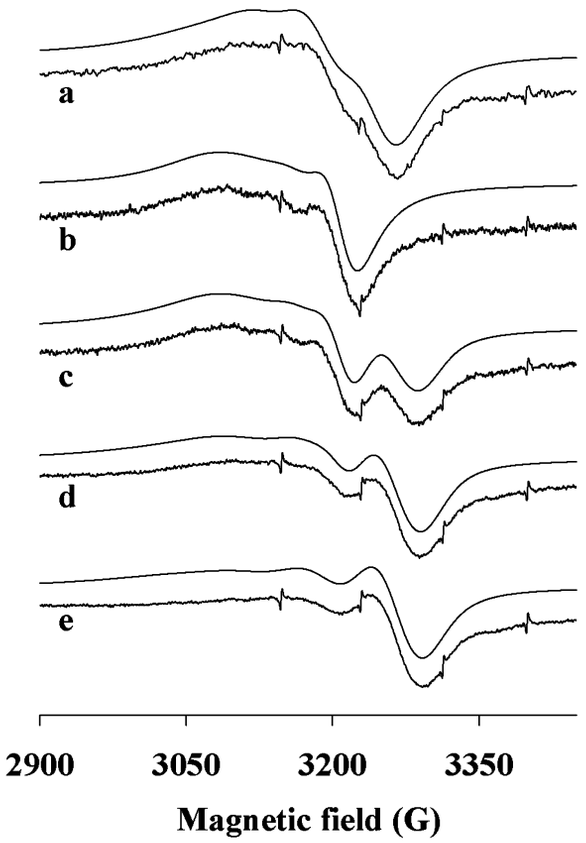

Fig. 5 Experimental and simulated EPR-spectra of the bimhm–copper(II) system. pH = 3.00 (a), 6.45 (b), 5.71 (c), 6.50 (d) and 8.21 (e). [L] = [M] = 0.005 M (a,b), [L] = 3 × [M] = 0.015 M (c–e), T = 298 K.

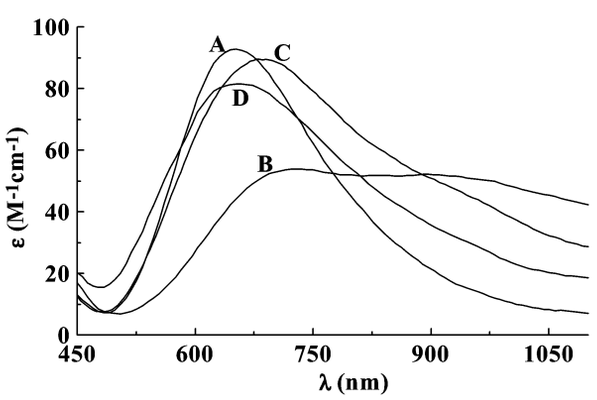

Fig. 6 Individual electronic absorption spectra of the main species formed in the bimhm–copper(II) system. **A**: CuLH, **B**: CuL, **C**: CuL_2H and **D**: CuL_2.

protonated second ligands (CuL + LH_x = CuL_2H_x, log K = 2.34 (x = 2), 2.96 (x = 1), 3.90 (x = 0)) are much lower than those of the first ligand. Their EPR and VIS spectra (Fig. 5 and 6) are characteristically different from those of $[Cu(bimhm)]^{2+}$, and indicate tetragonal geometry around the metal ion, though a weak low energy shoulder around 900–950 nm can still be observed. The important (110 and 65 nm) red shift of their d–d transitions, as compared to the analogous bis-complexes of imhm, suggests rather strong axial nitrogen co-ordination. Consequently, the above cited relatively low binding strength of the second ligand is due to a structural rearrangement during its co-ordination. Although the EPR spectra are consistent with the formation of bis-complexes, the individual parameters of the three co-existing bis-complexes could not be determined, owing to their very similar equatorial plane. The observed spectra can be well described with the superposition of CuL and another virtual species having four equatorial nitrogen donors around copper(II). The calculated concentration ratios of the two species are in good agreement with the ratio of CuL and the sum of the three bis-complexes determined on the basis of pH-metric titrations.

Some representative ^{1}H NMR spectra of the zinc(II)–bimhm system are depicted in Fig. 7. In equimolar solution, a new set

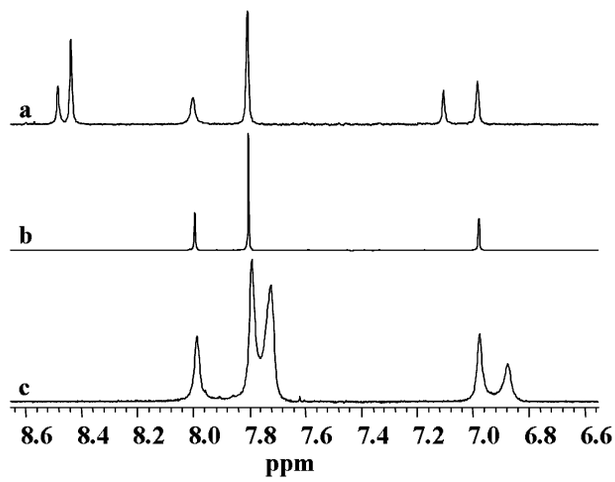

Fig. 7 Parts of the ^{1}H NMR spectra measured in the bimhm–zinc(II) system. [L] = [M] = 0.006 M, pH = 3.60 (a); [L] = [M] = 0.006 M, pH = 6.80 (b); [L] = 2 × [M] = 0.012 M, pH = 7.27 (c).

of signals appeared above pH 3, parallel with the formation of $[Zn(bimhm)]^{2+}$, indicating its slow ligand exchange on the NMR timescale. At pH 3.6 the signals of the imidazole rings in the complex are remarkably shifted upfield compared to those of the free ligand, as a result of their metal-promoted deprotonation. The formation of $[Zn(bimhm)]^{2+}$ induces important shifts of the CH_2 signals, too. Moreover, the singlet of the two (Im)–CH_2-groups splits into a typical AB type quartet upon complex fomation. The magnetic inequivalency of the methylene protons is due to the tetradentate co-ordination of bimhm, hindering the free rotation around the C–C/N bonds. In contrast with the zinc(II)–imhm system, the ligand exchange is slow on the NMR timescale even above pH 6–7, which is probably the result of the tetradentate nature of bimhm. Using two fold ligand excess, the observed spectrum is consistent with the presence of ZnL and the free ligand (Fig. 7c), in agreement with the pH-metric data.

The absence of zinc(II)-containing bis-complexes merits some discussion, since the 6N co-ordinated complexes are generally more favored in the case of zinc(II). Our preferred interpretation is a geometrical difference between the species $[Cu(bimhm)]^{2+}$ and $[Zn(bimhm)]^{2+}$. The square pyramidal $[Cu(bimhm)]^{2+}$ complex, with the bridgehead nitrogen in one of the basal positions, seems to transform easily into an octahedral species through the substitution of an equatorial imidazole nitrogen by the second ligand. The trigonal bipyramidal $[Zn(bimhm)]^{2+}$ species, with the bridgehead nitrogen in the apical position, is less susceptible to the co-ordination of a second ligand.

Conclusion

The new unsymmetrical imidazole-based tripodal ligand displays different geometrical preferences in the complexes $[Cu(bimhm)]^{2+}$ and $[Zn(bimhm)]^{2+}$. The square pyramidal copper(II) complex is able to form bis-complexes with similar distorted octahedral structure as the tridentate constituent of bimhm. In contrast, the trigonal bipyramidal $[Zn(bimhm)]^{2+}$ complex does not co-ordinate a second ligand under the conditions used. The $[CuL]^{2+}$ complex of the tridentate ligand imhm undergoes a deprotonation above pH 8, forming a

mononuclear hydroxo- and imidazolate-bridged oligonuclear complexes, existing in concentration dependent equilibrium.

Acknowledgements

This work was supported by the Hungarian Research Foundation (OTKA T025114 and OTKA T032929) and the Foundation of Research Development at Universities (FKFP 0109/2000).

References

1 S. Chen, J. F. Richardson and R. M. Buchanan, *Inorg. Chem.*, 1994, **33**, 2376.
2 L. P. Wu, Y. Yamagiwa, I. Ino, K. Sugimoto, T. Kuroda-Sowa, T. Kamikawa and M. Munakata, *Polyhedron*, 1999, **18**, 2047.
3 N. Wei, N. N. Murthy, Z. Tyeklár and K. D. Karlin, *Inorg. Chem.*, 1994, **33**, 1177.
4 K. J. Oberhausen, R. J. O'Brian, J. F. Richardson and R. M. Buchanan, *Inorg. Chim. Acta*, 1990, **173**, 145.
5 E. Quiroz-Castro, S. Bernes, N. Barba-Behrens, R. Tapia-Benavides, R. Contreras and H. Nöth, *Polyhedron*, 2000, **19**, 1479.
6 C.-Y. Su, B.-S. Kang, T.-B. Wen, Y.-X. Tong, X.-P. Yang, C. Zang, H.-Q. Liu and J. Sun, *Polyhedron*, 1999, **18**, 1577.
7 G. J. A. A. Koolhaas, W. L. Driessen, J. Reedijk, J. L. van der Plas, R. A. G. de Graaff, D. Gatteschi, H. Koojiman and A. L. Spek, *Inorg. Chem.*, 1996, **35**, 1509.
8 G. J. A. A. Koolhaas, P. M. van Berkel, S. C. van der Slot, G. Mendoza-Diaz, W. L. Driessen, J. Reedijk, H. Kooijman, N. Veldman and A. L. Spek, *Inorg. Chem.*, 1996, **35**, 3525.
9 H. Nie, S. M. J. Aubin, M. S. Mashuta, R. A. Porter, J. F. Richardson, D. N. Hendrickson and R. M. Buchanan, *Inorg. Chem.*, 1996, **35**, 3325.
10 C. Place, J.-L. Zimmermann, E. Mulliez, G. Guillot, C. Bois and J.-C. Chottard, *Inorg. Chem.*, 1998, **37**, 4030.
11 I. Török, T. Gajda, B. Gyurcsik, G. K. Tóth and A. Péter, *J. Chem. Soc., Dalton Trans.*, 1998, 1205.
12 I. Török, P. Surdy, A. Rockenbauer, L. Korecz, G. J. A. A. Koolhaas and T. Gajda, *J. Inorg. Biochem.*, 1998, **71**, 7.
13 T. Gajda, R. Krämer and A. Jancsó, *Eur. J. Inorg. Chem.*, 2000, 1635.
14 A. Jancsó, T. Gajda, E. Mulliez and L. Korecz, *J. Chem. Soc., Dalton Trans.*, 2000, 2679.
15 C. C. Tang, D. Davalian, P. Huang and R. Breslow, *J. Am. Chem. Soc.*, 1978, **100**, 3918.
16 K. Várnagy, I. Sóvágó, K. Ágoston, Zs. Likó, H. Süli-Vargha, D. Sanna and G. Micera, *J. Chem. Soc., Dalton Trans.*, 1994, 2939.
17 K. D. Karlin, P. L. Dahlstrom, M. L. Stanford and J. Zubieta, *Chem. Soc., Chem. Commun.*, 1979, 465; K. D. Karlin, P. L. Dahlstrom, J. R. Hyde and J. Zubieta, *Chem. Soc., Chem. Commun.*, 1980, 906.
18 R. W. Hay, T. Clifford and P. Lightfoot, *Polyhedron*, 1998, **17**, 4347.
19 A. M. Dittler-Klingemann, C. Orvig, F. E. Hahn, F. Thaler, C. D. Hubbard, R. van Eldik, S. Schindler and I. Fábián, *Inorg. Chem.*, 1996, **35**, 7798.
20 F. Thaler, C. D. Hubbard, F. W. Heinemann, R. van Eldik, S. Schindler, I. Fábián, A. M. Dittler-Klingemann, F. E. Hahn and C. Orvig, *Inorg. Chem.*, 1998, **37**, 4022.
21 R. H. Holm, P. Kennepohl and E. I. Solomon, *Chem. Rev.*, 1996, **96**, 2239.
22 F. J. C. Rosotti and H. Rosotti, *The determination of stability constants*, McGraw-Hill Book Co., New York, 1962, p. 149.
23 E. Högfeldt, *Stability Constants of Metal-Ion Complexes, Part A. Inorganic Ligands*, Pergamon, New York, 1982, p. 32.
24 L. Zékány and I. Nagypál, in *Computational Methods for the Determination of Formation Constants*, ed. D. J. Leggett, Plenum, New York, 1991.
25 A. Rockenbauer and L. Korecz, *Appl. Magn. Reson.*, 1996, **10**, 29.
26 E. Prenesti, P. G. Daniele, M. Prencipe and G. Ostacoli, *Polyhedron*, 1999, **18**, 3233.
27 M. Wienken, B. Lippert, E. Zangrando and L. Randiacco, *Inorg. Chem.*, 1992, **31**, 1985.
28 T. Gajda, B. Henry and J.-J. Delpuech, *J. Chem. Soc., Dalton Trans.*, 1993, 1301.
29 T. Gajda, B. Henry and J.-J. Delpuech, *Inorg. Chem.*, 1995, **34**, 2455.
30 P. G. Daniele, O. Zerbinati, V. Zeleno and G. Ostacoli, *J. Chem. Soc., Dalton Trans.*, 1991, 2711.
31 N. Matsumoto, Y. Motoda, T. Matsuo, T. Nakashima, N. Re, F. Dahan and J.-P. Tuchagues, *Inorg. Chem.*, 1999, **38**, 1165.
32 M. Q. Ehsan, Y. Ohba, S. Yamauchi and M. Iwaizumi, *Bull. Chem. Soc. Jpn.*, 1996, **69**, 2201.
33 K. D. Karlin, J. C. Hayes, S. Juen, J. P. Hutchinson and J. Zubieta, *Inorg. Chem.*, 1982, **21**, 4106.
34 M. Duggan, N. Ray, B. Hathaway, G. Tomlinson, P. Brint and K. Pelin, *J. Chem. Soc., Dalton Trans.*, 1980, 1342.
35 D.-H. Lee, N. N. Murthy and K. D. Karlin, *Inorg. Chem.*, 1997, **36**, 5785.
36 N. Wei, N. N. Murthy and K. D. Karlin, *Inorg. Chem.*, 1994, **33**, 6093.